Preshaping Profiler for Flexible Spacecraft Rest-to-Rest Maneuvers

Toshio Kamiya, Ken Maeda, and Naoto Ogura (*1)
Tatsuaki Hashimoto, Shin-ichiro Sakai (*2)

*(*1) NEC TOSHIBA Space Systems, Ltd., Fuchu, Tokyo, 183-8551, Japan*
*(*2) JAXA-ISAS, Sagamihara, Kanagawa, 229-8510, Japan*

Abstract: A new feedforward algorithm for flexible spacecraft maneuvers is presented. We call this preshaping profiler the nil-mode-exciting (NME) profiler. This algorithm is designed particularly for single-axis rest-to-rest rotational maneuvers (switching maneuvers) with linear actuators. Generally spacecraft with large flexible structure has a lot of large-mass flexible-modes. Therefore, uncertainity of high-order modes needs to be considered for high-accuracy controller design. This paper presents an extra-insensitive maneuvering method which overcomes above-mentioned difficulties. This algorithm includes a preshaping profiler formulated from sampling function (also known as sinc function), consequently feedforward control inputs generated from the preshaping profiler have no frequency response above a certain designed frequency. Therefore residual vibration at the end-point of maneuver can be highly reduced with minimum loss of maneuver agility.

Keywords: Attitude control, Flexible structure, Attitude Maneuver, Preshaping profiler, Flexible mode

柔軟衛星高速マヌーバ用の周波数事前成形プロファイラ

摘要：柔軟衛星の高速マヌーバのための新しいフィードフォワード制御アルゴリズム（NME プロファイラと称する）を提案する。大型柔軟構造物を有する衛星の姿勢マヌーバのためには柔軟物の固有振動数の不確定性に対するロバスト性が重要であり、大型構造物の場合、多数の大有効質量の柔軟モードを有するため、過去に提案された方式ではロバスト性確保が難しい場合が多い。提案する NME プロファイラは、コントローラと柔軟構造モードの理想的な周波数分離を可能とし、これらの欠点を克服する周波数事前成形プロファイラである。

I. Introduction

This paper is concerned with the problem of generating feedforward control inputs for flexible spacecraft, robotic manipulator, and pointing system, which are often required to maneuver as quickly as possible without significant structural vibrations after a maneuver.

Many researches have been examined about such a maneuvering problem. Most researchers propose algorithms based on feedforward bang-bang control with constant-force discrete actuators[1-6]. However, there are some drawbacks to these algorithms.

First, feedforward bang-bang control algorithms are generated from formulation of input shaping as a zero placement algorithm that can give rise to negative shapers. Negative input shapers have notch-shaped or bandpass-shaped frequency characteristic, so these input shapers are sensitive to modeling errors, and small modeling errors lead to significant amount of residual vibrations. In other words, negative shapers do not work well on most real systems because the system frequencies need to be known very accurately[1].

Second, negative input shapers consist of limited number of positive and negative constant-amplitude impulses, so these algorithms are effective for systems with finite number of flexible-modes. This can be restated in such a way that real flexible spacecraft usually has a lot of flexible-modes which are varied by each rotational axis, so negative input shapers can cause considerable amount of residual vibrations which originate from inescapable flexible-modes.

Third, constant-force discrete actuators such as on-off reaction jets are usually used as bang-bang control actuators. This implies low accuracy of control inputs compared to linear continuous actuators such as CMGs or RWs. This is mainly because on-off reaction jet is naturally inferior to CMG or RW in output torque accuracy.

This paper presents a preshaping profiler that overcomes above-mentioned drawbacks. The preshaping profiler has the function of computing maneuvering profiles for feedforward control inputs. This preshaping profiler is generated from extra insensitive functions which are called sampling function (also known as sinc function). Sampling function is known to be insensitive to frequencies above a designed one. This preshaping profiler significantly reduces residual vibrations at the end-point of maneuvers. The reason is as follows. First, residual vibrations are generated only as homogeneous solutions of satellite dynamic-equations if there are no control inputs after the maneuvers (control inputs exist in only maneuvering durations). Second, the homogeneous solutions can be disappeared if there are no structural frequencies in the frequency range of preshaping profiler. In consequence, all the residual vibrations in the end-point of maneuvers can be reduced by the preshaping profiler. This preshaping profiler also has high robustness to modeling errors, and this preshaping profiler is effective for systems with infinite number of flexible-modes. The reason is as follows. This preshaping profiler has lowpass-shaped frequency characterictic, hence, this causes no residual vibrations as long as flexible-modes exist in higher frequency than a certain frequency (sampling function frequency). This preshaping profiler is effective for high-accuracy control of satellites or manipulators or pointing systems with large complicated flexible structure.

This paper is organized as followings. Section II shows the outline of the controller. Section III defines preshaping profiler. Section IV shows effectiveness of this preshaping profiler compared to past methods.

Section V describes the outline of VSOP2(ASTRO-G) attitude control subsystem (i.e., ACS) which uses the proposed preshaping profiler, and application example to VSOP2(ASTRO-G) maneuvers is shown.

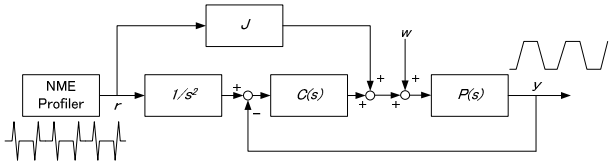

Fig. 1 Block diagram of ACS controller (VSOP2(ASTRO-G))

II. Outline of the Controller

The block diagram of ACS controller for VSOP2(ASTRO-G) is shown in Fig. 1. It consists of the feedforward control part of the nil-mode-exciting (NME) profiler and feedback control part of *C*. The input-output relation from the reference signal *r* and disturbance *w* to the measurement output *y* is given by

$$y = G_{yr} r + G_{yw} w \tag{1}$$

where

$$G_{yr} = G_{yw}(J + C/s^2), G_{yw} = (I + PC)^{-1} P \tag{2}$$

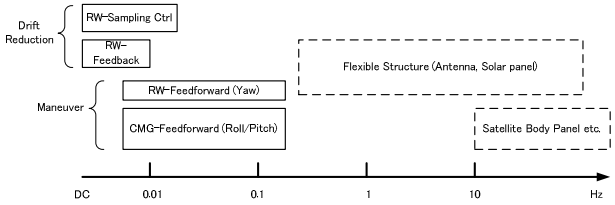

Fig. 2 Frequency assignments of each controller (VSOP2(ASTRO-G))

P denotes the plant transfer function. J denotes the spacecraft moment of inertia. We design *C* so that the closed-loop system is robustly stable and has disturbance attenuation capability to *w*. NME profiler generates the feedforward profile of the attitude maneuvers.

Fig. 2 shows the frequency assignments of each controller. Feedforward profiler (NME profiler) has higher frequency characteristic up to just below the 1st flexible mode. Feedback controller *C* has lower frequency and is used only for attenuating the attitude drift which is generated in long-time constant.

Because of this frequency separation between feedforward profiler (NME profiler) and feed back controller *C*, the characteristic of the NME profiler is not changed by the effect of feedback controller *C*. In the next chapter, we explain how to design the NME profiler.

III. Preshaping Profiler for Flexible Spacecraft

It is known that the shortest path of large angle rotational maneuvers is performed by means of single-axis rotation. The single axis is called *Euler-axis*. The Euler-axis is the only axis determined from initial attitude and final attitude.

This paper presents a maneuvering method of rotating around the Euler-axis (we are concerned here with spacecraft maneuver and not concerned with robotic manipulator and pointing system).

Sampling function (also known as *sinc function*) is defined as

$$y(t) = \frac{\sin(\omega_s t)}{\omega_s t}. \tag{3}$$

This function has no frequency response above ω_s.

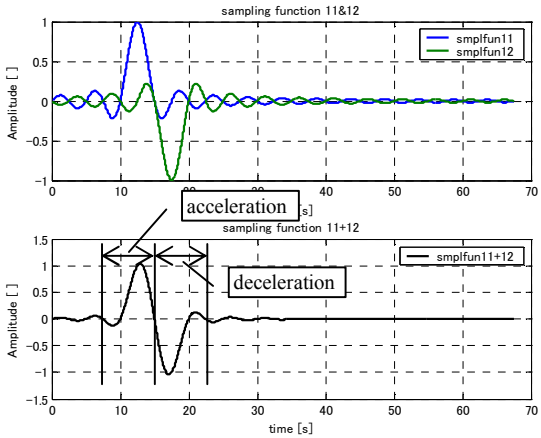

Fig. 3 Sampling function (upper) and combined sampling function (lower)

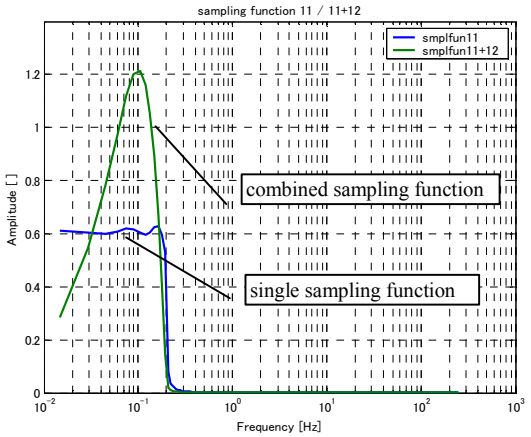

Fig. 4 Sampling function (frequency characteristic)

It is possible to separate frequency characterictic of ACS and flexible structures completely by means of sampling function. Fig. 3 shows overplot of two sampling functions (upper figure, there are two waveforms which have 180deg offset and inverse form) and combination (addition) of these two waveforms (lower figure). Fig. 4 shows frequency characteristic of sampling function. As shown in blue solid line of Fig. 4, sampling function has in itself no response above a certain frequency (here, 0.2Hz) and flat response below the frequency, and as shown in green solid line of Fig. 4, this basic character is not changed by combination (addition) of sampling functions. Therefore residual vibrations of flexible structures at the maneuver end-point can be reduced to almost zero by means of sampling function. As a result, observation missions which are performed after each maneuvers can be performed effectively in the shortest time.

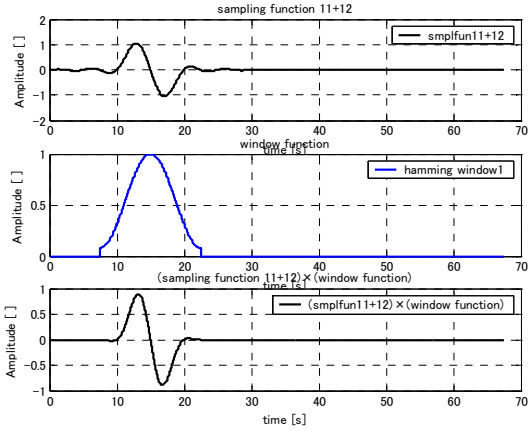

Fig. 5 Combined wave (upper – same as Fig. 3), window function (middle), and combined wave (lower)

To separate frequency characteristic of ACS and flexible structures, put the frequency of sampling function ω_s as

$$\omega_s < \omega_{flex}\Big|_{\text{lowest mode}} \tag{4}$$

where right-hand term is defined as the lowest flexible-mode frequency of the spacecraft.

Angular acceleration profile for control inputs is generated by addition of two sampling functions. As shown in upper figure of Fig. 3, there are two sampling functions in which peaks of these waves has offset of one period in time axis, positive wave is used for acceleration, negative wave is used for deceleration. Angular acceleration profile for control inputs is given by addition of these two waveforms. However, as lower figure of Fig. 3 shows, there are small waves left after deceleration, so it induces residual vibration of flexible structures. For this reason, a window function shown in middle figure of Fig. 5 is used to be added for smooth damping at the end-point of maneuvers. Lower figure of Fig. 5 shows angular acceleration profile for control inputs drawn by above procedure.

In this way, angular acceleration profile for back and forth rest-to-rest maneuvers is given as

$$\frac{d^2\theta(t)}{dt^2} = A\left\{ g_1(t)\left(\frac{\sin\left(\omega_{smpl}\left(t-t_{offset11}\right)\right)}{\omega_{smpl}\left(t-t_{offset11}\right)} - \frac{\sin\left(\omega_{smpl}\left(t-t_{offset12}\right)\right)}{\omega_{smpl}\left(t-t_{offset12}\right)} \right) + g_2(t)\left(\frac{\sin\left(\omega_{smpl}\left(t-t_{offset21}\right)\right)}{\omega_{smpl}\left(t-t_{offset21}\right)} - \frac{\sin\left(\omega_{smpl}\left(t-t_{offset22}\right)\right)}{\omega_{smpl}\left(t-t_{offset22}\right)} \right) \right\} \tag{5}$$

where θ is the body-angle based on the Euler-axis, A is the maximum acceleration, $t_{offset\,ij}$ is the offset time of each peaks, and g_k is the window function. Here, the offset time $t_{offset\,ij}$ are expressed as

$$t_{peakoffset} = t_s = \frac{2\pi}{\omega_s} \tag{6}$$

$$t_{mnv} = 3t_s \tag{7}$$

$$t_{offset11} = \frac{t_{mnv}}{2} + \frac{t_{obs}}{2} - \frac{t_{peakoffset}}{2} \tag{8}$$

$$t_{offset12} = t_{offset11} + t_{peakoffset} \tag{9}$$

$$t_{offset21} = t_{offset11} + t_{mnv} + t_{obs} \tag{10}$$

$$t_{offset22} = t_{offset12} + t_{mnv} + t_{obs} \tag{11}$$

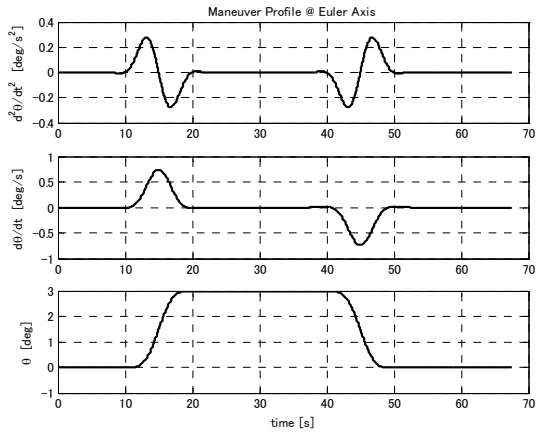

Fig. 6 Acceleration (upper), body-rate (middle), and body-angle (lower) profiles of a back and forth maneuver

where t_{mnv} is the maneuver time, t_{obs} is the observation time.

The window functions g_k are hamming window which expressed as

$$g_i(t) = \begin{cases} 0.54 + 0.46\cos\left(\dfrac{2\pi}{t_{win}}\left(t - \dfrac{t_{offset\,i1} + t_{offset\,i2}}{2}\right)\right) \\ \qquad \text{for} \quad \text{abs}\left(t - \dfrac{t_{offset\,i1} + t_{offset\,i2}}{2}\right) \le \dfrac{t_{win}}{2} \\ 0 \qquad \text{for} \quad \text{abs}\left(t - \dfrac{t_{offset\,i1} + t_{offset\,i2}}{2}\right) > \dfrac{t_{win}}{2} \end{cases} \tag{12}$$

where t_{win} is the time width of window function and equals to maneuver duration t_{mnv}. Fig. 6 shows a back and forth maneuvering profile computed from Eq. (5). We call this preshaping profiler the nil-mode-exciting (NME) profiler.

So far we have outlined the way in which angular acceleration profile is given. Now we would like to reconsider the purpose of this research. The main purpose is to perform rest-to-rest maneuver of flexible spacecraft in the shortest time with linear actuators. For that purpose, such maneuvers described below are necessary.

[1] with a profile that does not cause residual vibrations (Transient vibrations during maneuvers have no influence on mission performance)

[2] make the most of torque output performance of the actuator

Item [1] can be achieved by the characteristic of the angular acceleration profile which is generated by the NME profiler. As shown in Fig. 4, the angular acceleration profile has no frequency response above a certain designed frequency ω_s. Consequently, the profile does not cause steady-state vibrations after the attitude maneuvers.

As to item [2], as shown in upper figure of Fig. 3, there are two sampling functions in which these waves has a time offset, and positive wave is used for acceleration, negative wave is used for deceleration. Angular acceleration profile is defined by addition of these two waveforms. Here, for the maximum uses of the actuator ability, the peak of the angular acceleration profile A should be set to the angular acceleration that

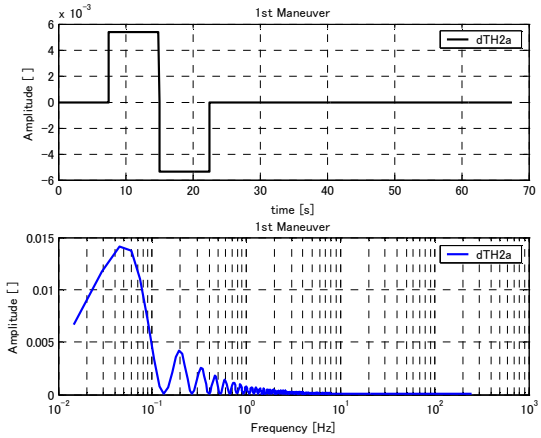

Fig. 7 Acceleration profile (upper) and frequency characteristic (lower) of the past method[7]

is computed from the maximum torque of the actuators. This is how [2] is achieved.

In addition, a window function is combined with sampling functions. This purpose is to reduce residual vibration after maneuvers caused as particular solution of satellite dynamic-equations with minimum loss of the advantages of [1] and [2].

IV. Evaluation of NME Profiler

The effectiveness of the nil-mode-exciting (NME) profiler compared to a past method is shown as follows. Fig. 7 shows maneuver profile given by a past method[7]. The profiler of this method proposes the maximum acceleration and the maximum deceleration profiles during maneuvers. Since frequency separation of ACS and flexible structures is not considered in this past method as shown in lower figure of Fig. 7, excitation of

flexible-modes cannot be avoided. Therefore, the observation mission can not be started until residual vibrations damp sufficiently. In other words, this maneuver needs longer time to complete.

Open-loop dynamics simulations using these methods are performed for 3 [deg] rest-to-rest maneuvers. Each simulation is performed on the same conditions which include the same flexible satellite and same actuator performances. Table 1 shows major parameters for analyses. Desired maneuver profiles generated by each method are shown in Fig. 8 and Fig. 9. Open-loop dynamics simulation results are shown in Fig. 10 and Fig. 11. The antenna gain-losses are calculated as the sum square of flexible-modes displacements. So magnitude of the residual vibrations can be estimated by antenna gain-losses. As shown in Fig. 10, residual vibrations after maneuver of the past method do not damp for long time. On the other hand, as shown in Fig. 11, residual vibrations at the end-point of maneuver of the NME profiler are reduced to almost zero. The effectiveness of NME profiler was verified by open-loop dynamics simulations.

V. Application to VSOP2(ASTRO-G)-ACS

In this section, application to VSOP2(ASTRO-G)-ACS is introduced. VSOP2(ASTRO-G) (VSOP: VLBI Space Observatory Programme) is a satellite which includes 2-CMGs and 4-RWs as control actuators. Missions of VSOP2(ASTRO-G) are performed by way of back and forth rest-to-rest high speed maneuvers (switching maneuvers) in which the same couple of target celestial sources are pointed repeatedly. The satellite attitude is required to be highly-stable at the end-point of maneuvers. Fig. 12 shows on-orbit image of VSOP2(ASTRO-G). This satellite has two kinds of flexible appendages, large deployable antenna and flexible solar panel.

The feature of this system exists in the part of NME profiler that computes the best profile of feedforward control inputs in which the character frequencies of the flexible appendages are not excited.

Condition for the switching maneuver analysis is 3[deg]/15[s]. Figure 13 shows the body angle errors which are calculated as the differences between evaluation results and target body angle. Each error is within acceptable level.

Table 1 Conditions for analyses

items	conditions
maneuver angle	3 [deg]
maneuver time	15 [s]
CMG rotor momentum	60 [Nms]
CMG max. torque	42 [Nm]/2CMG

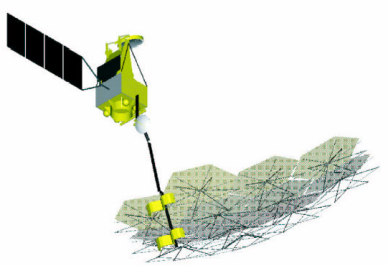

Fig. 12 VSOP2(ASTRO-G) on-orbit image

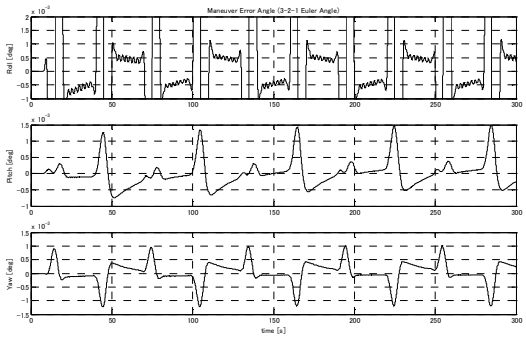

Fig. 13 Body angle errors

VI. Conclusion

A new approach for computing feedforward control inputs for flexible spacecraft rest-to-rest maneuvers was proposed. The effectiveness, robustness, and expandability of this preshaping profiler was confirmed. Ideal frequency separation was realized between flexible-modes and controllers.

Acknowledgments

This research was supported by all the members of VSOP2(ASTRO-G) team in JAXA-ISAS and NEC TOSHIBA Space Systems, Ltd.

The methods described in this paper are patent pending. Commercial use of these methods requires written permission from JAXA-ISAS and NEC TOSHIBA Space Systems, Ltd.

References

[1]Singhose, W. E., Seering, W. P., and Singer, N. C., "Time-Optimal Negative Input Shapers," *ASME J. Dynam. Syst. Meas. Control*, Vol. 112, 1997, pp. 198-205.

[2]Singer, N. C., Seering, W. P., "Preshaping Command Inputs to Reduce System Vibration," *ASME J. Dynam. Syst. Meas. Control*, Vol. 112, 1990, pp. 76-82.

[3]Singhose, W., Derenzinski, S., and Singer, N., "Extra-Insensitive Input Shapers for Controlling Flexible Spacecraft," *AIAA J. Guid. Control Dynam.* Vol. 19, 1996, pp. 385-391.

[4]Liu, Q., Wie, B., "Robust Time-Optimal Control of Uncertain Flexible Spacecraft," *AIAA J. Guid. Control Dynam.* Vol. 15, 1992, pp. 597-604.

[5]Singh, G., Kabamba, P. T., and McClamroch, N. H., "Planar, Time-Optimal, Rest-to-Rest Slewing Maneuvers of Flexible Spacecraft," *AIAA J. Guid. Control Dynam.* Vol. 12, 1989, pp. 71-81.

[6]Singh, G., Kabamba, P. T., and McClamroch, N. H., "Bang-Bang Control of Flexible Spacecraft Slewing Maneuvers: Guaranteed Terminal Pointing Accuracy," *AIAA J. Guid. Control Dynam.* Vol. 13, 1990, pp. 376-379.

[7]Saito, T., Maeda, K., Ninomiya, K., and Hashimoto, T. H., "Rate-Profiler Based Minimum-Time Control for Spacecraft Attitude Maneuver," *IFAC Proceedings of 15th IFAC Symposium on Automatic Control in Aerospace*, 2001, pp. 83-88.

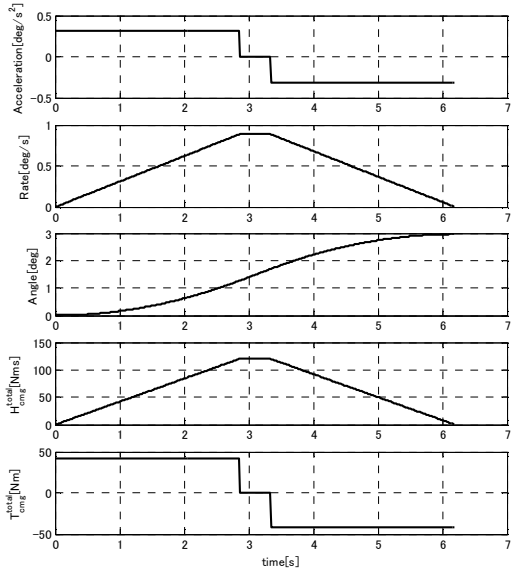

Fig. 8 Maneuver profiles of the past method[7]

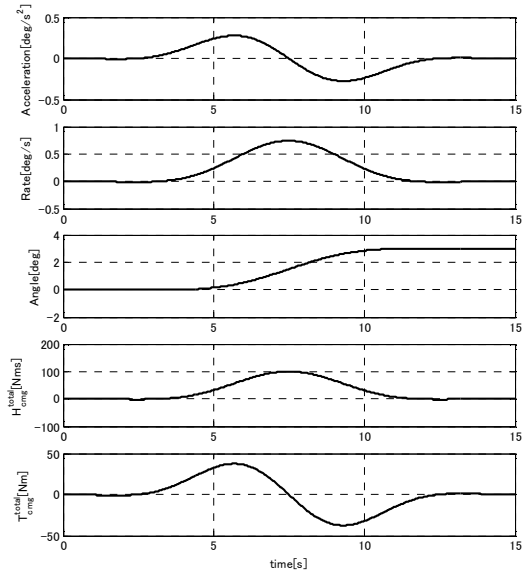

Fig. 9 Maneuver profiles of the NME profiler

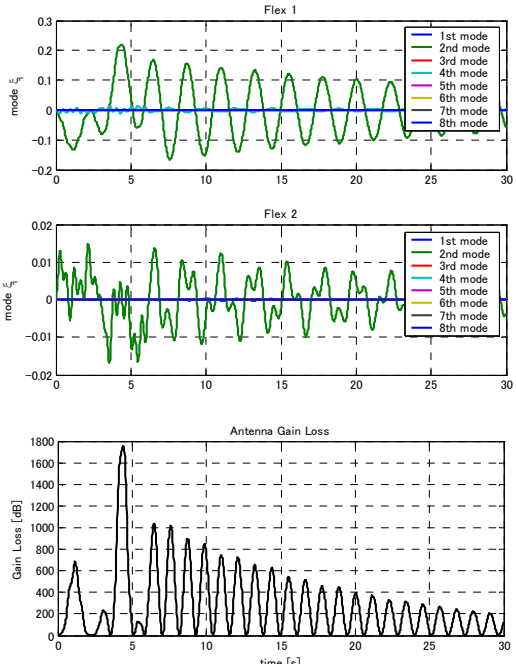

Fig. 10 Dynamics simulation of the past method[7]

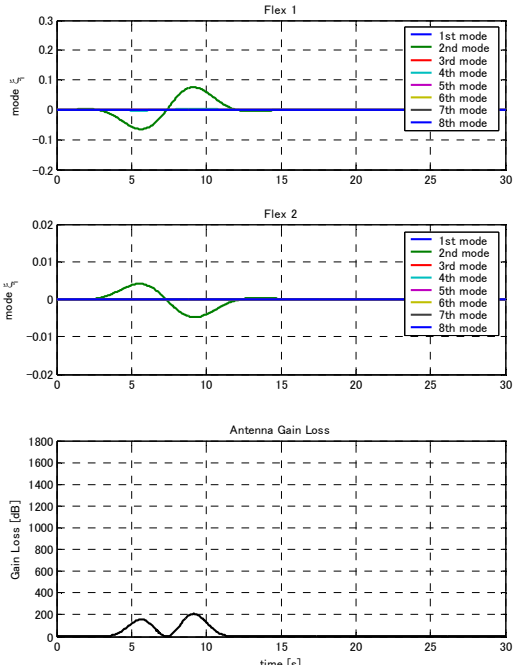

Fig. 11 Dynamics simulation of the NME profiler